Effect of Cellular Deadhesion on Endosomal Recycling in HeLa Cells

A thesis submitted in partial fulfilment of the requirements for the award of the degree of

MASTER OF SCIENCE

By

Aritra Mondal

17MS168

Under the supervision of

Dr.Bidisha Sinha

Department of Biological Sciences

Indian Institute of Science Education and Research, Kolkata

May 2022

Declaration

I, Aritra Mondal, 17MS168, a student of the Department of Biological Sciences of the BS-MS Dual Degree Program of IISER Kolkata, hereby declare that this thesis is my own work and, to the best of my knowledge, it neither contains materials previously published or written by any other person, nor it has been submitted for any degree/diploma or any other academic award anywhere before.

I also declare that all copyrighted material incorporated into this thesis is in compliance with the Indian Copyright (Ammendment) Act, 2012 and that I have obtained permission from the copyright owners for my use of their work.

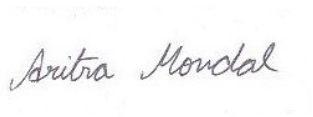

Aritra Mondal
17MS168
Department of Biological Sciences
Indian Institute of Science Education and Research, Kolkata
Mohanpur, West Bengal - 741246, India

Certificate

Date: 24-05-2022

This is to certify that the thesis titled "Effect of Cellular Deadhesion on Endosomal Recycling in HeLa cells", submitted by Aritra Mondal (17MS168), a student of the Department of Biological Sciences of the BS-MS Dual Degree Programme of IISER Kolkata, is based upon his own research work under my supervision. I also certify, to the best of my knowledge, that neither the thesis nor any part of it has been submitted for any degree/diploma or any other academic award anywhere before. In my opinion, the thesis fulfils the requirement for the award of the degree of Master of Science.

Dr. Bidisha Sinha
Associate Professor
Department of Biological Sciences
Indian Institute of Science Education and Research, Kolkata
Mohanpur, West Bengal - 741246, India

Acknowledgements

This study would not have been possible without the expertise of Dr. Bidisha Sinha, our beloved guide, who helped me to plan out the project and constantly provided her guidance and valuable time, throughout the duration of my study.

My sincere thanks also goes to Dr. Arnab Gupta for providing the plasmids for my experiments.

A debt of gratitude is owned to my laboratory colleagues and seniors, especially Tithi Mandal, who helped me with the culture and transfection of HeLa cells and also guided me to plan and carry out the experiments. Thanks also goes to Tanmoy Ghosh, for continuously helping me in experiments and with writing codes for Image Analysis. I had a really wonderful time working with Subhendu Chatterjee, Madhura Chakraborty, Ananya Biswas, Jibitesh Das, Upasana, Alekhya, and Nanditha , who always motivated me with their insightful discussions.

I would like to extend my gratitude to IISER Kolkata, for letting me use the Confocal Microscope in the Central Imaging Facility and also to Mr. Ritabrata Ghosh, who helped me a lot during imaging of my samples.

I would like to thank all my friends and seniors in IISERK, for being like a family to me. I am very grateful to Biswanath Saha, who mentored me through all my academic and non-academic experiences, in the last 5 years. Finally, I want to thank my parents, Purabi and Abhijit Mondal, and my extended family, for always believing in me, and providing me with whatever I needed.

ARITRA MONDAL

Contents

Abstract

Regulation of membrane tension is crucial for the large-scale coordination of cell boundary dynamics. A bidirectional flow of lipids in the form of endosomes, between the plasma membrane and the endosomal pool helps to maintain this steady-state condition. However, cells undergoing mechanical processes like deadhesion often change their shape from a flat spread out state to a rounded shape, reducing the tension of the membrane. In response to this sudden change, cells respond by tweaking the rates of endocytosis and exocytosis, such that excess membrane can be moved away from the membrane and homeostasis is achieved. Previous studies have shown that the temporal evolution of membrane tension during deadhesion, might be oscillatory. In this study, we have tried to investigate the dynamics of this regulation of tension by the endocytic machinery, using fluorescence microscopy to quantify the intracellular population of the endosomes. We have also built a computational model of the endocytic recycling system, which can describe the relative membrane tension for different conditions.

Objectives

The objectives of this study are-

1. To quantify and study intracellular population of early and recycling endosomes, during deadhesion.
2. To understand how membrane tension is regulated by processes like endocytosis and exocytosis.
3. To understand the evolution of tension profile during cellular deadhesion.
4. To build a computational model for the endocytic recycling system.

Chapter 1

INTRODUCTION

1.1 Endocytosis

Endocytosis is the cellular process by which all kinds of extracellular cargo like food, solute molecules, ligands and other membrane components are delivered to different intracellular destinations. It is also important for the regulation of major functions like Antigen presentation and for activating intracellular signaling cascades. The transmembrane proteins and ligands delivered by endocytosis mediate necessary cellular functions and responses to external stimuli. As a result, endocytosis is a highly regulated process and consists of a large number of different pathways. Disregulation of these pathways can lead to a multitude of physiological, immunological and neuro-degenerative diseases including Parkinson's Disease and Alzheimer's Disease[1]. So, a complete understanding of this complex network of pathways is critical to our understanding of a huge array of cellular processes. Endocytosis also holds therapeutic potential which include targeted drug delivery to intracellular destinations and development of methods to combat pathogens and toxins that misuse this system.

1.2 Pathways of Endocytosis and Exocytosis

There are several endocytic pathways responsible for the endocytosis of different types of cargo to the cell. These pathways can be broadly categorised into - Clathrin Mediated Endocytosis (CME) and Clathrin Independent Endocytosis (CIE). CME has been extensively studied in the past and it has been found to be involved in the cellular up-

take of nutrients and growth factor receptors[2,22]. It is the most dominant pathway of endocytosis in the cell, with estimates suggesting that it can contribute upto 95% of the total amount of endocytosis occuring in the cell[3]. Being such a major pathway, it can also be exploited by pathogens such as influenza virus[4] and bacterial toxins like Shiga toxin[5].

CIE, on the other hand, comprises of multiple distinct endocytic pathways. It facilitates both small scale processes and large micrometer scale pathways like macropinocytosis and phagocytosis. Some of these pathways are dependant on dynamin, while others utilize the actin machinery for membrane remodeling[6,7]. Examples of CIE are Caveloae Mediated Endocytosis, the CLIC-GEEC pathway and Arf6-Associated pathway[8]. The dynamin independant, CLIC-GEEC pathway has been discussed in details, further in the report.

These pathways are responsible for the internalization of cargo in the form of vesicles, which are essentially small sections of the plasma membrane. The cargo internalised via these pathways eventually fuse and lead to a larger vesicular (or tubular) structure called the Early Endosome. Here, the cargo is sorted according to their target destinations. The internalized ligands are degraded and sorted into late endosomes and eventually to the lysosomes[9]. The receptors, however, can either be returned to the plasma membrane by recycling or sent to the lysosomes for degradation along with the ligands[10].

The recycling of the receptors along with membrane back to the plasma membrane is called exocytosis, and is equally important to maintain the proper composition of the plasma membrane. This is achieved by multiple recycling pathways from the endocytic machinery. Major pathways include fast recycling from vesicles, sorting of cargo from early endosomes and recycling using recycling endosomes, and maturation of early endosomes into ERC and formation of tubular recycling endosomes[11].

1.3 Rab proteins

Rab's are the largest family of small Ras-like GTPases, which regulate the transport of cargo in the endocytic machinery. They are involved in all the steps of endocytic pathways like vesicle budding, membrane fusion, maturation, degradation and recycling[24].

Over 60 different Rab GTPases are associated with the intracellular membranes in humans[12]. It is the disregulation or alteration in Rab proteins, that disrupts the endocytic machinery and leads to neurological disorders and mental retardation in humans.

Rab proteins can act as molecular switches by cycling between an inactive GDP-bound state and an active GTP-bound state. This activation of Rab's from the GDP-bound state to GTP-bound state is carried out by a guanine nucleotide exchange factor or GEF. Another protein called the GTPase-activating protein or GAP can then hydrolyse the GTP-bound Rab and lead to its inactivation[13]. The Rab effectors can only bind to the Rab in its GTP-bound state and not the GDP-bound state. This is called the Rab cycle.(Figure-1.1(B))

In the early endocytic pathway, Rab5 regulates clathrin-coated-vesicle-mediated transport from the plasma membrane to the early endosomes as well as homotypic early endosome fusion. Some of the endocytosed membrane is recycled directly to the PM by the Rab4 mediated fast recycling pathway. The rest of the cargo is sorted into different compartments which either mature and move inside the cell or are recycled back in a Rab4 dependent pathway. These pathways marked by Rab4 and Rab5 are the pathways that we will investigate in this study. The aforementioned pathways are depicted in a schematic below(Figure-1.1(A)).

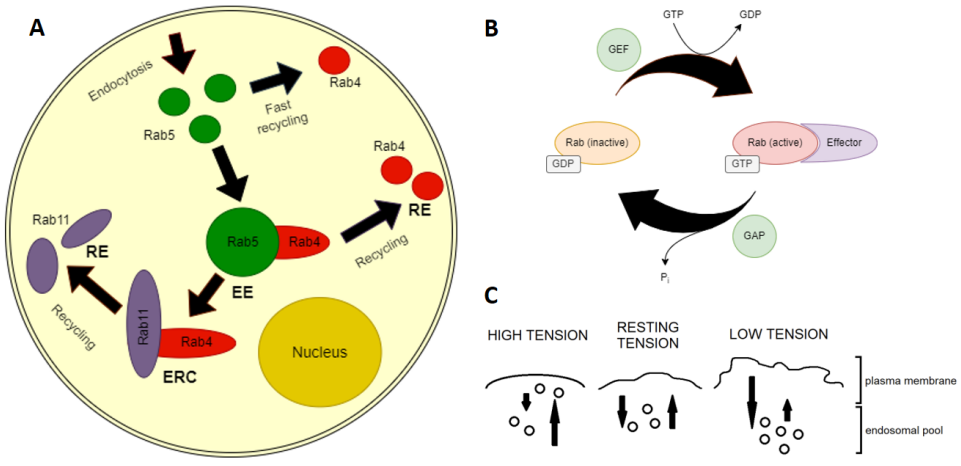

Figure 1.1: **(A)** Localization of different Rab proteins in the endocytic recycling pathway, **(B)** The Rab cycle, **(C)** Relationship between Plasma Membrane tension and rates of endocytosis(up-arrow) and exocytosis(down-arrow). Size of arrow is proportional to rates

1.4 How does Endosomal Recycling affect Cell Membrane Tension?

Endocytosis is a significant housekeeping process, performed actively by the cell. The endocytic recycling pathway is capable of recycling more membrane than the content of the cell membrane itself, within hours[14]. So, these processes have a major impact on the landscape of the plasma membrane, merely because of the amounts of membrane they transport. As a result, these pathways are highly regulated in a complex network, to maintain smooth flow of cargo between inside and outside the cell.

The bidirectional flow of membrane also helps to maintain the physical parameters of the membrane, like the PM tension. An increased rate of endocytosis causes more membrane to be internalized, resulting in a reduced pool of membrane in the PM. As a result, the PM transitions to a more stretched state, which corresponds to a higher tension value. Similarly, increasing the rate of exocytosis brings extra membrane back to the PM, thereby reducing the tension[15]. So, the endocytic recycling pathway can also act as a regulator of membrane tension(Figure-1.1(C)).

1.5 Cellular Deadhesion and Surface Area Regulation

Cellular deadhesion is the process by which a flat and spread-out cell, adhered to the substrate, detaches from the substrate, completely or partially. This is achieved by the restructuring of stress fibres and cleaving the focal adhesions of the cell. In both cases, rounding of the cell is observed, upto varying degrees.

Cell rounding lowers the tension of the cell membrane as the surface area of the rounded state is lower than the surface area of the stretched cell. This results in the accumulation of more membrane than is required to maintain membrane tension homeostasis. Cells have various strategies to compensate this sudden change in membrane tension, one of which is to increase the rate of endocytosis, such that the excess membrane can be moved to the endosomal pool. This endocytosed membrane can then be either recycled back by exocytosis or degraded in lysosomes.[23,26]

So, clearly processes like cellular adhesion and deadhesion change the tension profile of the cell membrane rapidly. The interconnection of cellular adhesion and membrane

tension has been well studied in the past, but the effects caused by deadhesion is still largely unknown.

Cellular deadhesion can be induced in adherent cells by treatment with Trypsin. Another commercially available cell-dissociation reagent is TrypLE (*Gibco*).

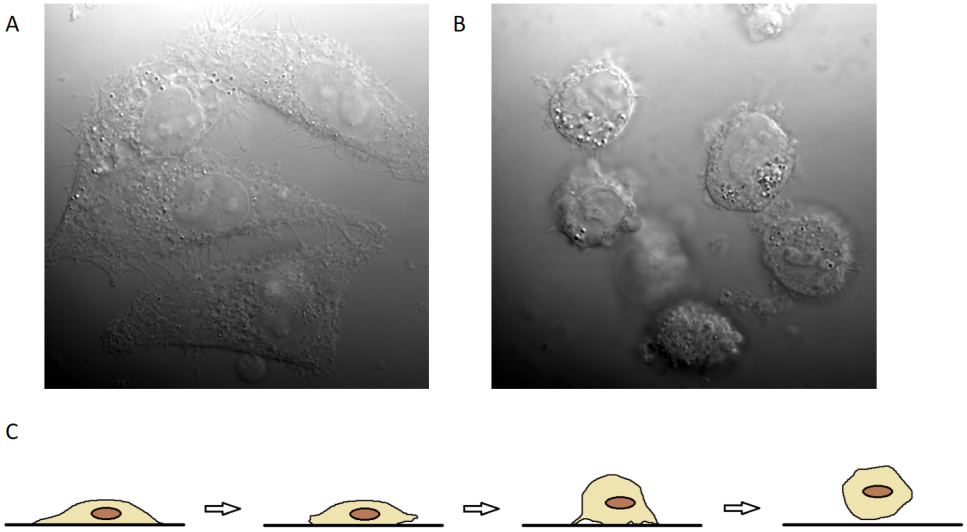

Figure 1.2: Representative DIC images of HeLa cells in **(A)** adhered state , **(B)** Deadhered state after trypsin-induced deadhesion, **(C)** Schematic of Cellular Deadhesion

1.6 The CLIC-GEEC Pathway

The CLIC/GEEC or CG pathway is a CIE pathway with primary carriers called CLathrin-Independent Carriers (CLICs). These CLICs mature into tubular early endosomal compartments called Glycosylphosphotidylinositol- anchored protein (GPI-AP) enriched compartments or GEECs. The CG pathway requires the actin polymerization machinery for endocytosis, which is recruited by the cholesterol sensitive protein, cdc42[16].

The CG pathway is a pinocytic pathway and accounts for major uptake of fluid and bulk membrane in many cells. About 40% of the endocytosed fluid is recycled within 5 minutes. This ability to quickly internalize and recycle large chunks of membrane enables it to carry out processes like membrane repair and homeostasis[17,18,25,27].

Chapter 2

MATERIALS AND METHODS

2.1 System of Study

HeLa cell line were chosen for this study. Extensive data and standardized protocols for experiments is available for this cell line. From the literature survey, we found out that this is the most common cell line used for experiments on endocytosis, among human cell lines.

2.2 Cell Culture and preparation

HeLa cells were grown in Dulbecco's Modified Essential Medium (DMEM, *Gibco, Life Technologies, USA*) with 10% fetal bovine serum (FBS, *Gibco, HI, US origin*) and 1% anti-anti (*Gibco*) at 95% humidity, 5% CO2 and 37°C. Cells were then seeded in round glass bottom dishes and maintained in growth media. The initial cell count per dish, during seeding was roughly 10^5.

2.2.1 Protocol for Coverslip Etching

(a) Dip in 1:19 glacial acetic acid : 95 % ethanol for 15 minutes.

(b) Dip in 95 % ethanol for 30 minutes.

(c) Dip in 100 % ethanol for at least 15 minutes.

2.2.2 Protocol for Dish Preparation for Cell Culture

(a) Take 35mm dishes with a hole at the centre and dip in 70 % ethanol for several hours for cleaning.

(b) Take out the required number of dishes and etched cover slips and keep it on a tissue paper for drying.

(c) Paste one cover slip at the base of each dish using silica gel from a syringe.

(d) Seed roughly 10^5 cells at the centre of the coverslip and add 2mL media.

(e) Incubate for 18-24 hrs at 37 °C.

2.3 Co-transfection

Cotransfection refers to transfection with two separate nucleic acid molecules on the same cell. Lipofectamine 3000(*Life Technologies*) transfection reagent was used for the co-transfection of EGFP-Rab5 plasmid DNA (Addgene plasmid:49888) and mCherry-Rab4 plasmid DNA (Addgene plasmid:55125). Cells were co-transfected at a confluency of about 70 % and then incubated for 16 hours at 37°C.

2.3.1 Protocol for Co-Transfection

For every dish requiring 40 µL of DNA-transfection reagent mix,

(a) Add 0.5 µL of each DNA to an eppendorf tube.

(b) Add 2 µL P3000 reagent to it and dilute in 17 µL OptiMEM.

(c) In another eppendorf, dilute 2 µL Lipofectamine 3000 in 18 µL OptiMEM.

(d) Prepare both the solutions and incubate at Lab Temperature for 5 mins.

(e) Add the contents of both the eppendorfs and incubate at Lab Temperature for 20 mins.

(f) Carefully add 40 µL co-transfection reagent at the centre of the culture dishes.

2.4 Pharmacological Treatments

Cells were treated with various drugs and reagents which selectively inhibit certain pathways of endocytosis.

2.4.1 Protocol for ATP Depletion

ATP Depletion suppresses almost all ATP-dependent active pathways of endocytosis, but not the ATP-independent passive pathways. So, most pathways of endocytosis are suppressed.

(a) Add 10 mM sodium azide (Sigma) and 10 mM 2-deoxy D-glucose (Sigma) to M1 Imaging medium (150 mM NaCl (Sigma), 1 mM MgCl2 (Merck), and 20 mM HEPES (Sigma))

(b) Replace media with 2mL of ATP Depletion media and incubate for 60 mins.

(c) Discard media from dishes and wash 3 times with filtered PBS.

2.4.2 Protocol for dynasore treatment

To study the effect of inhibition of the dynamin-dependent pathways of endocytosis, dynasore, a small molecule inhibitor of dynamin was used. Dynamin helps in the pinching off of the vesicles from the plasma membrane, which are formed by different pathways. Dynasore reversibly inhibits the GTPase activity of dynamin, inhibiting the pinching off of vesicles. Dynasore only inhibits GTP hydrolysis but now the affinity for GTP binding or dynamin self-assembly, itself. As a result, pits still form in a dynasore treated cell, but these are not cleaved off from the membrane.

(a) Take the co-transfected dishes and discard media.

(b) Add 2 mL of glucose-free media to serum-starve the cells and incubate at 37 °C.

(c) For every dish, take 1.25 µL dynasore (80 µM) and add it to 2mL serum-free media.

(d) Take the dishes out from incubator and replace media with dynasore-added media. Incubate for 20 mins.

(e) Discard media from dishes and wash 3 times with filtered PBS.

2.4.3 Protocol for ML141 treatment

Similarly, to study the effect of inhibition of the CLIC-GEEC pathway, a CIE pathway of endocytosis, we treat the cells with ML141, which inhibits cdc42 protein. As a result of this inactivation, actin polymerization machinery necessary for endocytosis using this pathway is not recruited.

(a) Take the co-transfected dishes and discard media.

(b) Add 2 mL of glucose-free media to serum-starve the cells and incubate at 37 °C.

(c) For every dish, take 0.61 µL ML141 (10 µM) and add it to 2mL serum-free media.

(d) Take the dishes out from incubator and replace media with ML141-added media. Incubate for 30 mins.

(e) Discard media from dishes and wash 3 times with filtered PBS.

2.4.4 Protocol for trypsin treatment to induce deadhesion

After these treatments, the cells were treated with trypsin, which induces deadhesion in adherent cells. 0.25% trypsin was added for 0 minutes (control), 3 minutes and 6 minutes in separate dishes.

(a) Prepare 0.25% trypsin and add suitable amounts of endocytosis- inhibiting drugs to it, as per the experiment requirement.

(b) Among the 6 dishes per experiment, choose 1 dish each from control and drug-treated samples and mark them t0.

(c) Choose another pair of dishes (1 from control and 1 from treated) and replace the media with the trypsin prepared earlier.

(d) Use a stopwatch to keep track of time and remove the trypsin exactly after 3 minutes of its addition.

(e) Wash with PBS 2 times.

(f) Repeat last 3 steps with the last pair of dishes, but with 6 mins of trypsin application instead of 3 mins.

(g) Discard media from dishes and wash 3 times with filtered PBS.

2.4.5 Protocol for Fixation

The cells are then fixated using Paraformaldehyde solution, which....

(a) To make 4% PFA in PBS, add 2g PFA to 50 mL filtered PBS and leave in hot air oven at °C overnight.

(b) Add 2 mL, 4% PFA in PBS, to the dishes and incubate at RT(21 °C) for 15 mins.

(c) Wash with PBS 2 times.

(d) Apply parafilm, wrap in aluminium foil and store at 4 °C for imaging within 3 days.

2.5 Image Acquisition

2.5.1 Confocal Microscopy

A Confocal Laser Scanning Microscope or CLSM uses movable mirrors and a pinhole to direct a thin focused beam of light, by which it can scan the sample pixel by pixel, both in the same plane and in different planes. The issue with conventional fluorescence microscopes is that fluorescent light from adjacent planes of the focal plane also enter the objective resulting in a very noisy image. The presence of a pinhole, which allows only the central part of the defocused beam to enter the objective, solves this issue and results in images with very little noise.

The samples were first observed under an epifluoresence microscope (IX81, *Olympus*) to check for successful co-transfection. Imaging was performed using a confocal Microscope (CLSM710, *Zeiss*), with a Plan-Apochromat 100x/1.4 Oil DIC M27 objective. Excitation lines were set at 488nm and 561nm for GFP and mCherry channels, respectively. Z-stacks were collected at 460 nm slice intervals with a resolution of 512 × 512 pixels(16-bit). The pinhole size was set to 93µm and the pixel size was 166µm. Scan averaging was set to 2 per pixel.

10 cells were selected and imaged as z-stacks from each dish. The average time to capture 1 z-stack image was roughly 7-10 mins (Acquisition time: 7.75 seconds/frame). Additionally, about 20 snapshots of the perinuclear region(2-5 µm from base of cell) of cells were also taken from each dish. These images were saved in (.lsm) format and exported for analysis.

2.5.2 Image Analysis

Images were analysed using the computer softwares, ImageJ(v1.53) and MATLAB(R2021a). Additionally, the programming language, Python was used to handle .csv data files and Origin was used for plotting.

The freehand tool in ImageJ was used to draw "region of interests" (**roi**), by manually tracing over the boundary of the cells. Individual roi's were drawn for each slice of the z-stack and saved. These roi files along with the image files are used as input for a MATLAB code used for endosome counting. This code is able to detect endosomes based on intensity thresholding and object detection and generates data in .csv files, which can be further processed.

The parameter, 'endosome area fraction' refers to the total endosome area (over a single slice or zstack) of detected endosomes, divided by the spread area (slice or zstack) of the cell. It can be calculated separately for early and recycling endosomes, and internal and peripheral endosomes.

2.6 Computational Model

We have tried to model a very simple model of the endocytic recycling system, with only endocytosis and exocytosis occuring between the plasma membrane and the endosomal pool. The rates of both these processes can be varied as required, which would affect the membrane tension and surface area ratio of the cells. The movement of membrane in this model can be simulated using rate kinetics.

In this system, the lipid bilayer is considered as a rough-textured membrane with lots of microscopic bumps and invaginations along its surface. We can quantify two different types of surface areas of the cell- the Microscopic area (M) and the Spread Area (S). The Microscopic area is the sum total area of the membrane present in the folds and

invaginations, while spread area is the bulk approximate area of the cell, neglecting the microscopic irregularities. The Spread area can be thought of as the shadow or projection of the membrane, as is illustrated in Figure-2.1(b).

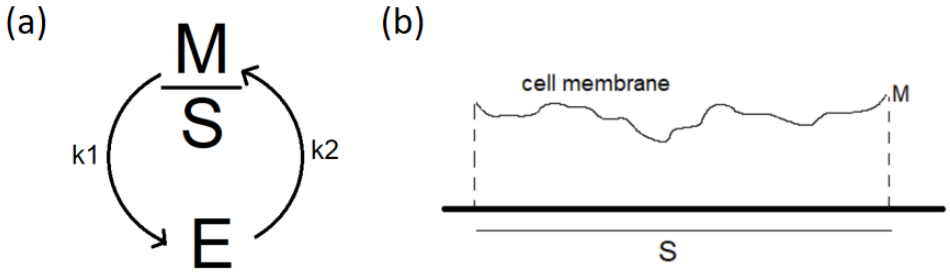

Figure 2.1: **(a)** An oversimplified model of endosomal recycling. k1 and k2 represent rates of endocytosis and exocytosis, respectively. **(b)** Microscopic area (M) and Spread area (S) of the cell

In this system, the rate of endocytosis (k1) depends inversely on the tension of the cell membrane. Whenever the membrane is more tensed, it would be more difficult to bend the already stretched membrane to form vesicles for endocytosis. As a result, the higher the membrane tension goes, the rate of endocytosis drops with it and vice-versa. Similarly, the rate of exocytosis is directly proportional to the membrane tension. The more tensed the membrane becomes, the more the cell will try to provide extra membrane to the PM by exocytosis.

The cell membrane tension is proportional to the ratio of the microscopic area (M) to the spread area (S) of the cell. We can write it as a quantity($\Delta A/A$) proportional to the ratio of the difference between M and S, and S. There is also a time delay (L) before a lipid molecule can be exocytosed back to the membrane after getting internalized. The spread area of the cell is kept constant in all cases, unless mentioned otherwise.

$$\frac{\Delta A}{A} = \frac{M - S}{S}$$

$$k_1 = \frac{\Delta A}{A} * c$$

$$M = microscopic\ Area,\ S = Spread\ Area,\ k_1 = endocytosis\ rate,\ c = constant$$

From the aforementioned conditions, we obtain a system of equations, defining the steady-state of the endocytic recycling pathway.

$$\frac{dM(t)}{dt} = -k_1 M(t) + k_2 E(t-L)$$

$$\frac{dE(t)}{dt} = k_1 M(t) - k_2 E(t-L)$$

$$\frac{dS(t)}{dt} = 0$$

$$M = microscopic\ Area,\ S = Spread\ Area,\ E = Endosomal\ Pool,\ t = time,\ L = lag$$

$$k1 = endocytosis\ rate,\ k2 = exocytosis\ rate$$

We start to simulate the system with initially chosen values of M, S, and E. The rates of k_1 and k_2 were varied relative to each other[29,30,32,33] and all other parameters were then fine tuned relative to these values.[31], The microscopic area is seen to reach a steady state value after a few damped oscillations. The oscillations are dependent on the values of k_1 and k_2. The effect of varying k_1 and k_2 on the Microscopic area is shown in Figure 2.2(A-B).

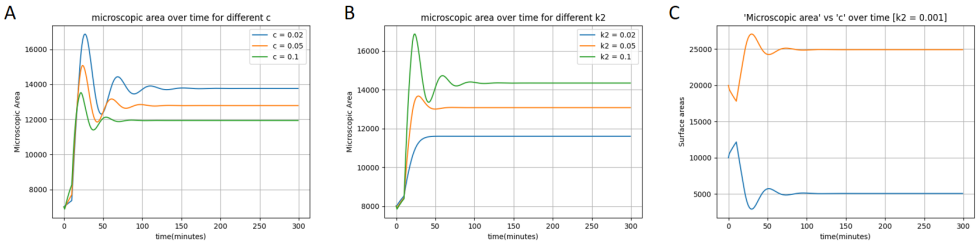

Figure 2.2: **(A)** Microscopic area over time for different values of k_1 (k_1 = (M/S - 1)*c. **(B)** Microscopic area over time for different values of k_2. **(C)** Amount of membrane in Microscopic area (orange) and Endosomal Pool(blue)

The microscopic area stabilizes at a lower value, as k_1 is increased. This means that for a higher rate of endocytosis, the M/S ratio will be lower, which indicates high tension. Meanwhile, the microscopic area stabilizes at a higher value, as k_2 is increased. The M/S ratio increases with k_2, indicating lower tension.

Figure 2.2(C) shows that the total amount of membrane present in M and E combined is a constant.

Chapter 3

Results

3.1 Effect of Trypsin induced Deadhesion on Endosomes

Cellular deadhesion can be quantified by the change in spread area in cells. Previous studies have found a characteristic sigmoid decrease in the spread area of cells, during deadhesion.

In our study, we observe a significant decrease in the spread area of HeLa cells, as shown in Figure-3.1. The basal slide(s) of the confocal images were manually selected and used to measure the spread area. In most cases, there is a sharp decrease of the spread area from (t=0min) to (t=3min). For (t=3min) to (t=6min), a decreasing trend is observed, although, not significant, for all cases.

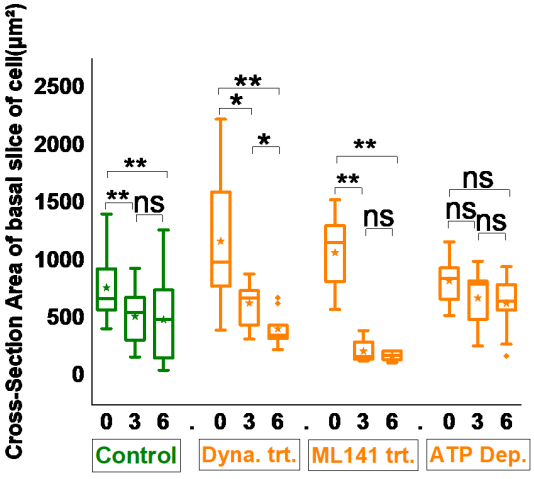

Figure 3.1: Spread area of cell for t0, t3 and t6 plates, for each condition. Labels in x-axis represent time in minutes for conditions. n=27(control), n=9(for treated)

3.2 Effect of Deadhesion on Early and Recycling Endosomes

Trpsin treatment resulted in a significant increase in the early endosomes, both internal and peripheral. A similar behaviour is observed in the internal recycling endosome pool. We also found a very significant increase of peripheral recycling endosomes from 0-3 mins, which then stabilizes and shows non significant change in 3-6 mins.

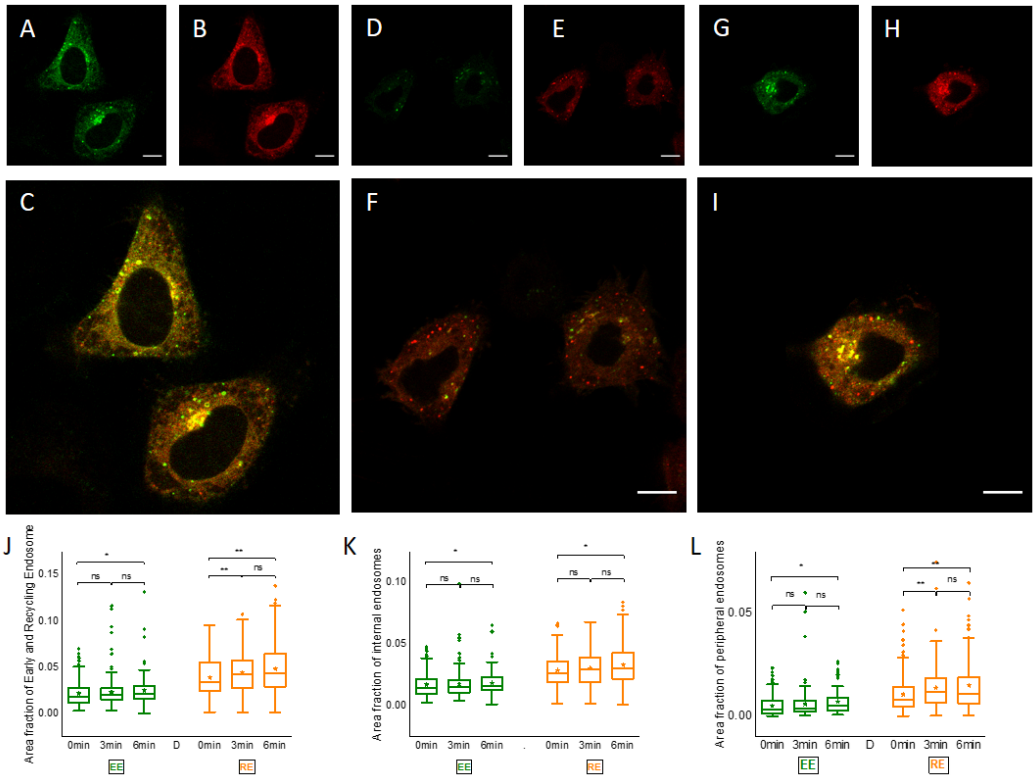

Figure 3.2: Effect of Trypsin Induced Deadhesion on HeLa cells. HeLa cells were co-transfected with Rab5-EGFP(green) and Rab4-mCherry (red) to mark Early endosomes (EE) and Recycling endosomes (RE), respectively. Representative images of Control cells **(A-C)** without trypsin treatment (t=0 min), **(D-F)** with 3 mins trypsin treatment (t=3 min), **(G-I)** with 6 mins trypsin treatment (t=6 min). Images **(C,F,I)** depict merged images from both channels at the three time points. **(J)** Area fraction of total EE and RE **(K)** Area fraction of internal EE and RE **(L)** Area fraction of peripheral EE and RE. Scale bar: A-10µm (all images) (N_{expt}=8, n_{cells}=180 per sample)

All these indicate an increased rate of endocytosis during deadhesion. With the progression of endocytosis, the different endosomal compartments start to show significant increase in their populations. As membrane starts to flow from the PM to the endosomal the lowered membrane tension is increased due to endocytosis. But after a lag,

exocytosis results in the lowering of tension and the cycle starts again. This gives rise to an oscillatory behaviour that dampens over time.

A schematic showing the various steps of our proposed model is given in Figure 3.3(A-D).

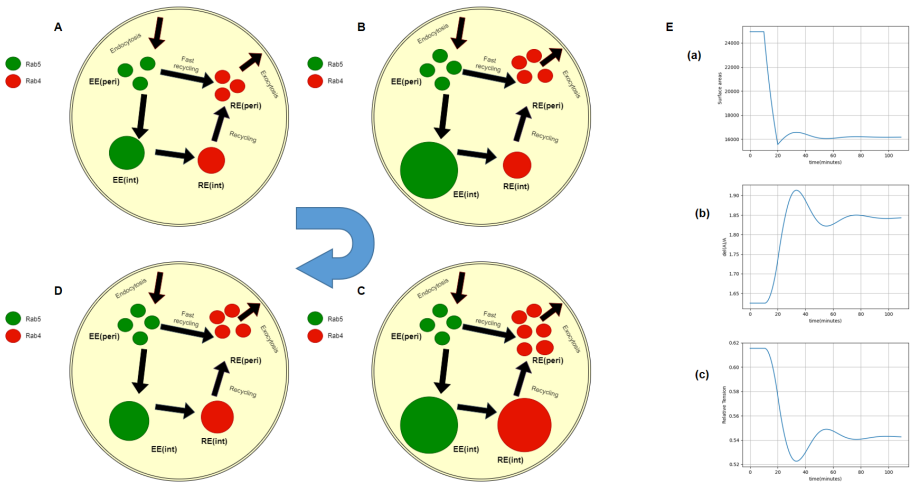

Figure 3.3: Proposed model of endocytic recycling during deadhesion. **(A)** Deadhesion leads to low membrane tension, which triggers endocytosis. Endocytosis of membrane increases the PM tension. **(B)** Increased endocytosis results in increase in peripheral EE population. Most of the membrane is transported to internal EE pool. Peripheral RE also increases due to fast recycling. **(C)** Recycling cargo is sorted from internal EE pool to internal RE pool. This results in more recycling, which reduces membrane tension. **(D)** The internal RE population quickly decreases due to recycling pathways. But, the lowered membrane tension caused by recycling again triggers more endocytosis. **(E)** Results of computational model of deadhesion. Effect of deadhesion over time on- **(i)** Microscopic Area **(ii)** $(\Delta A/A)$ **(iii)** Relative Tension of Membrane

To simulate deadhesion in our computational model, we reduce the spread area of the cell, with a rate k_3. This increases the M/S ratio and lowers tension(analogous to accumulation of excess membrane on PM). The effect of such condition on the Microscopic area, $(\Delta A/A)$, and relative tension is shown in Figure 3.3(E).

3.2.1 Colocalization of Rab4 and Rab5 in deadhering cells

Rab4 and Rab5 have been found to be present on the same endosomes, but in distinct domains of the membrane. Prescence of this intermediate endosome can be used to mark the rate of early to recycling endosome maturation. It can be measured as a ratio of the area of endosomes with Rab4 and Rab5 overlapping, to the total area of early endosomes (or recycling endosomes). Colocalization results of Rab4 and Rab5 is

illustrated in Figure 3.4.

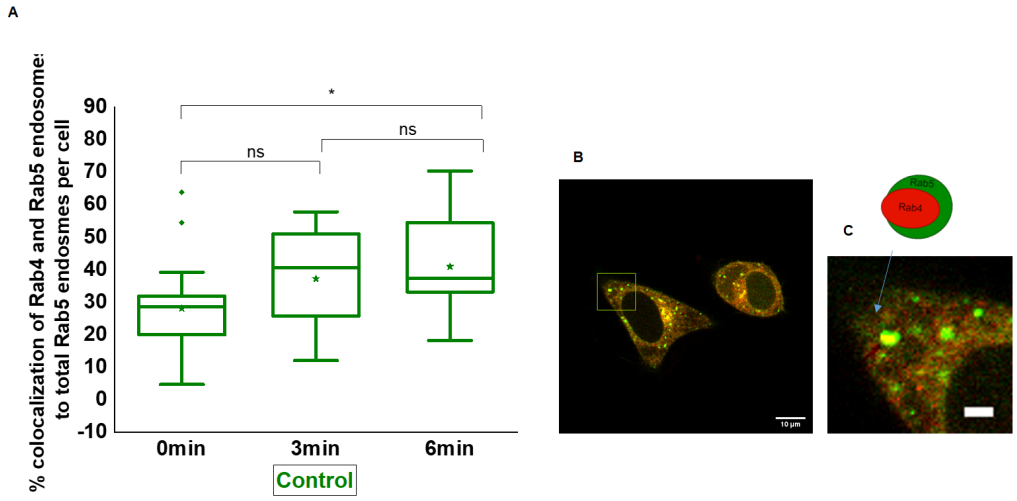

Figure 3.4: HeLa cells were co-transfected with Rab5-EGFP(green) and Rab4-mCherry (red) to mark Early endosomes (EE) and Recycling endosomes (RE), respectively. **(A)** %age colocalization of Rab4 and Rab5 to Rab5 EE. **(B)** Representative Image showing colocalization of Rab4 and Rab5 on endosomes. **(C)** Zoomed section of (B) with cartoon showing overlap of Rab proteins in same endosome

We find a significant increase of Rab4 and Rab5 colocalization from (t=0 mins) to (t=6 mins), which again marks an increase in the rate of endocytic recycling.

3.2.2 Spatial Distribution of Endosomes in the Cell

There is an increase in the rates of endocytosis and exocytosis during deadhesion. This results in more number of endosomes being generated from and fusing back to the PM. As a result, a large number of endosomes are present on the periphery of the cell, compared to the internal parts of the cell. Apart from this, the distribution of early and recycling endosomes on the z-axis (height) was also plotted. Most endosomes were found to be present in the basal part of the cell, where the actual deadhesion and change in tension occurs.

The distribution of endosomes on the z-axis is given in Figure 3.5.

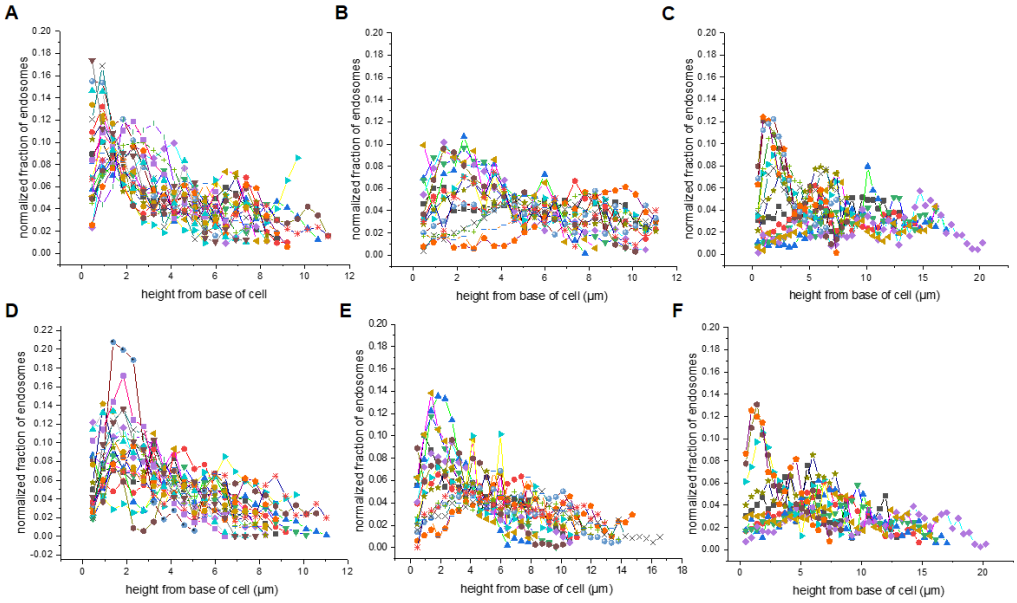

Figure 3.5: Distribution of early endosomes **(A-C)** and recycling endosomes**(D-F)** on the z-axis. x-axis in the plots represent normalized percentage of total endosomes per cell, and y-axis represents height along z-axis. Subfigures **A,D** represent (t=0 mins), **B,E** represent (t=3 mins) and **C,F** represent (t=6 mins)

The basal 5 slices of HeLa cells were found to contain 43.5%, 24.4%, and 25.8% of all early endosomes, at (t=0 mins), (t=3 mins), and (t=6 mins), respectively. Similarly, for recycling endosomes, the percentages were 41.8%, 27.5%, and 31.1%. This might indicate that the increased rate of endocytosis oscillates and eventually subsides with time, as the membrane tension stabilizes.

3.3 Effect of Deadhesion in ATP Depleted Samples

Most pathways of endocytosis require energy for carrying out the various steps like vesicle formation, pinching, actin assembly, etc all. As a result, ATP Depletion suppresses all major active pathways of endocytosis [19] . We have tried to study deadhesion in such a case where most of the endocytic pathways are supressed.

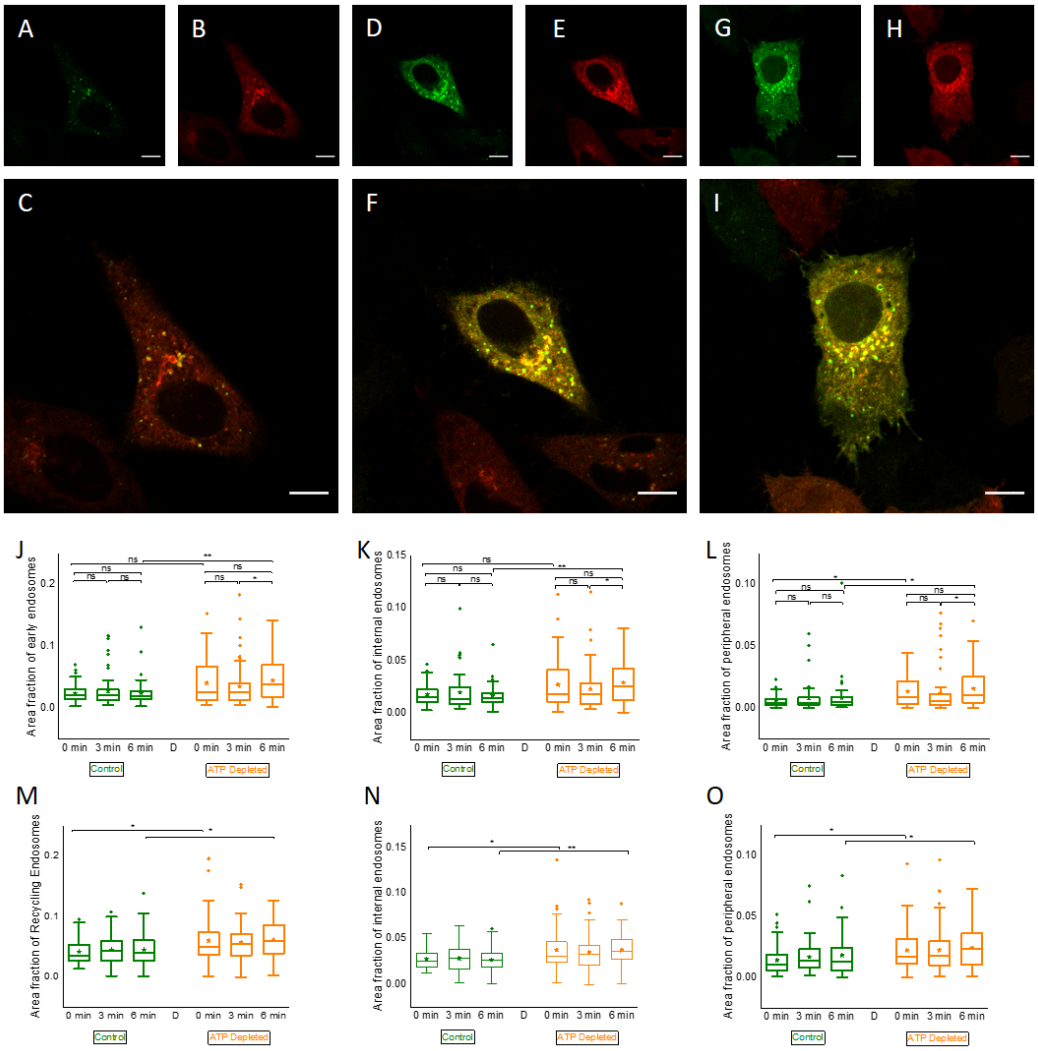

Figure 3.6: Effect of ATP Depletion on trypsinized HeLa cells. HeLa cells were co-transfected with Rab5-EGFP(green) and Rab4-mCherry (red) to mark Early endosomes (EE) and Recycling endosomes (RE), respectively. Representative images of ATP treated cells **(A-C)** without trypsin treatment (t=0 min), **(D-F)** with 3 mins trypsin treatment (t=3 min), **(G-I)** with 6 mins trypsin treatment (t=6 min). Images **(C,F,I)** depict merged images from both channels at the three time points. **(J)** Area fraction of total EE **(K)** Area fraction of internal EE **(L)** Area fraction of peripheral EE **(M)** Area fraction of total RE **(N)** Area fraction of internal RE **(O)** Area fraction of peripheral RE. Scale bar: A-10µm (all images) (N_{expt}=3, n_{cells}=60 per sample)

We did not observe any major changes in the endosomal populations, apart from an increase in the early endosomes at later stages of deadhesion (t=3 mins to t=6 mins).

However, an interesting observation was that ATP Depleted cells have more number of internal endosomes than control cells. This difference can be especially seen in the internal recycling endosome population. This can be due to the fact that ATP Depletion also suppresses the intracellular trafficking and maturation of endosomes. As a result, intracellular trafficking and maturation of endosomes take place at a very slow rate and endosomes get stuck at the recycling endosomal pool, before getting recycled.

Our proposed model for deadhesion in ATP Depleted cells is represented in a schematic in Figure 3.7.

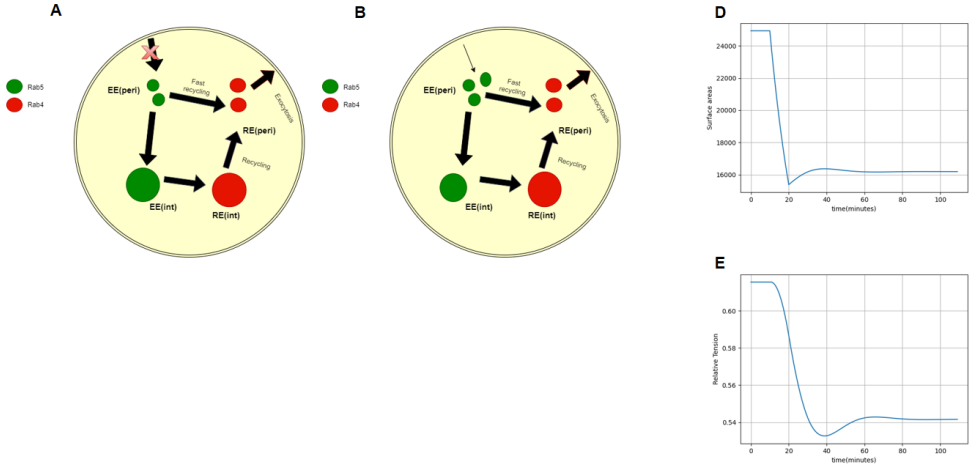

Figure 3.7: **(A)** ATP Depletion suppresses most pathways of endocytosis. So, even during deadhesion, the amount of membrane getting endocytosed will be very small. **(B)** B : Decreased endocytosis along with ATP Depletion result in no significant changes in the endosomal compartments. Although, a significant increase can be observed in the EEs after a delay. **(D-E)** Results of computational model of deadhesion in ATP Depleted cells. Effect of deadhesion over time on- **(D)** Microscopic Area **(E)** Relative Tension of Membrane

We reduce both the rates of k_1 and k_2, to simulate this system. We observed similar trends of microscopic area and relative tension values, except the oscillations were flattened out and with smaller amplitude. This indicates the occurence of deadhesion-induced endocytosis, although, at a much reduced rate.

3.4 Effect of Deadhesion in Dynamin-inhibited Samples

Dynamin is an important GTPase protein involved in the pinching off of vesicles from the PM. It spirals around the neck of vesicles/pits on the PM and performs a twisting or stretching action, causing membrane fission. It is involved in major endocytic pathways like CME and CavME.

Dynasore, an inhibitor of dynamin, inhibits the pinching off of vesicles from the PM, without any effect on pit formation. As a result, these pits can sometimes keep growing and form long tubules inside the cell[20,21,28], before eventually getting pinched off. So, dynamin can essentially inhibit or supress all dynamin-dependent pathways, including CME.

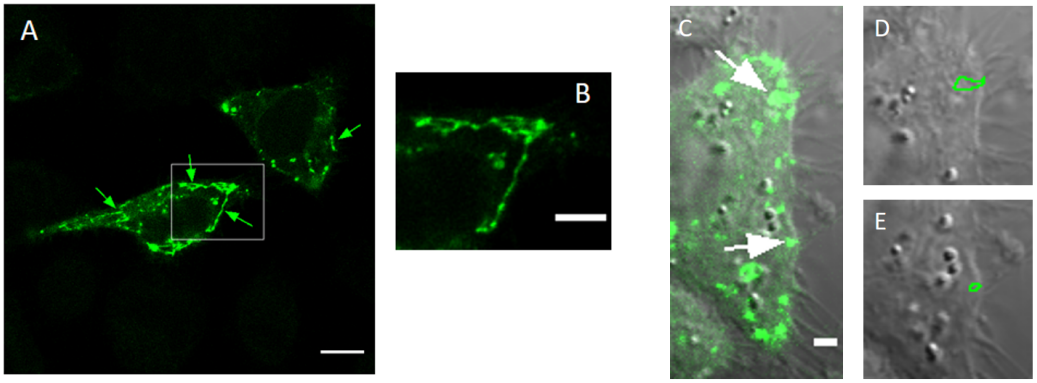

Figure 3.8: **(A-B)** Zoomed in view of tubules observed on dynasore treatment on HeLa cells. Arrows indicate Rab5-marked tubular structures. **(C)** Merged Rab5-EGFP and DIC. **D-E** Outlines of Early Endosomes drawn on DIC showing surface connected endosomes. Scale bar: A-10µm, B-5µm, C-2µm

For dynasore treated cells, we observe a significant increase in the number and amount of peripheral early endosomes, during early stages of deadhesion. A few cells with extensive surface connected tubules were also observed at later stages of deadhesion(Figure 3.8). There was no significant change in the internal EE pool.

The recycling endosomes, however show an initial increase in the peripheral endosomes, indicating increased recycling to the PM, in response to deadhesion. But thereafter, there is a decrease in the number of RE all over the cell, especially the internal pool. This might be caused due to an overall shortage of membranes in the entracellular pool of endosomes, as a large part of the membrane localizes in the surface-connected tubules, and cannot be used for endocytic recycling and tension regulation.

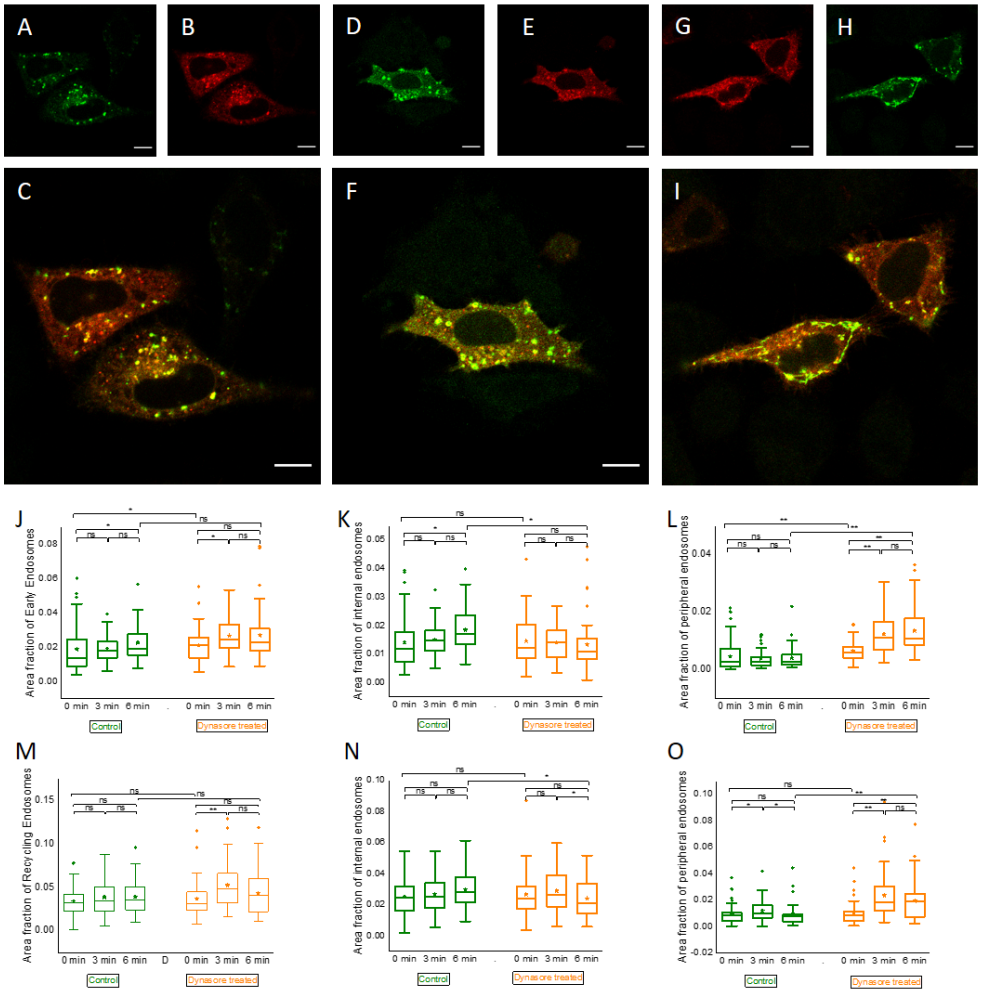

Figure 3.9: Effect of Dynamin Inhibition using Dynasore on trypsinized HeLa cells. HeLa cells were co-transfected with Rab5-EGFP(green) and Rab4-mCherry (red) to mark Early endosomes (EE) and Recycling endosomes (RE), respectively. Representative images of Dynamin treated cells **(A-C)** without trypsin treatment (t=0 min), **(D-F)** with 3 mins trypsin treatment (t=3 min), **(G-I)** with 6 mins trypsin treatment (t=6 min). Images **(C,F,I)** depict merged images from both channels at the three time points. **(J)** Area fraction of total EE **(K)** Area fraction of internal EE **(L)** Area fraction of peripheral EE **(M)** Area fraction of total RE **(N)** Area fraction of internal RE **(O)** Area fraction of peripheral RE. Scale bar: A-10µm (all images) (N_{expt}=3, n_{cells}=70 per sample)

As a consequence, the loss of functional membrane from the endocytic pathway, increases the tension of the cell membrane, to even higher values that the initial tension values, before deadhesion. (Figure 3.10(E))

A schematic with the various steps in our proposed model is given in Figure 3.10(A-D).

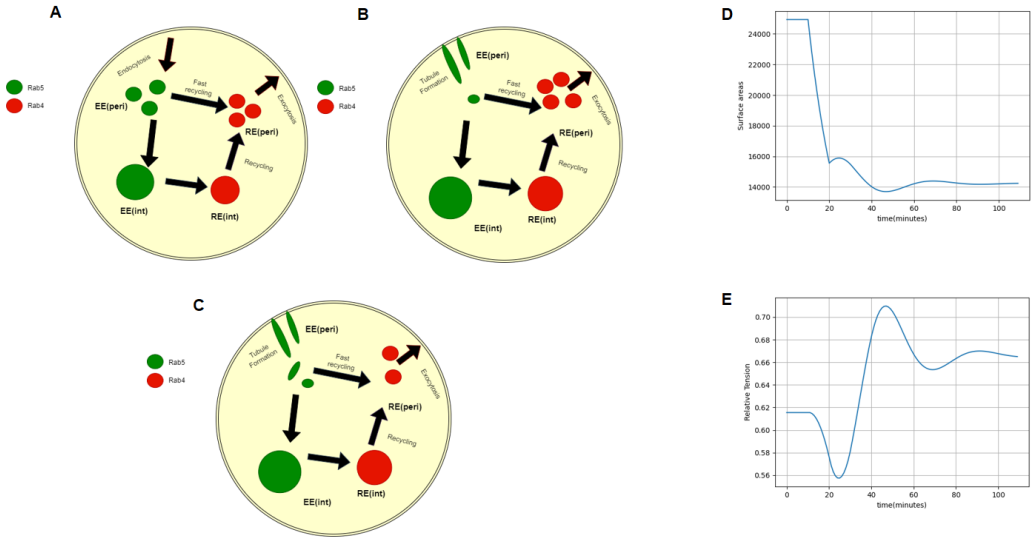

Figure 3.10: **(A)** Deadhesion leads to low membrane tension, which triggers endocytosis. Endocytosis of membrane increases the PM tension. **(B)** The vesicles formed by endocytosis cannot be pinched off from the PM due to dynamin inhibition. **(C)** Recycling cargo is sorted from internal EE pool to internal RE pool. This results in more recycling, which reduces membrane tension. **(D-E)** Results of computational model of deadhesion. Effect of deadhesion over time on- **(D)** Microscopic Area **(E)** Relative Tension of Membrane

To simulate dynasore treatment, we introduce a small change in our model. The rate of endocytosis and the amount of membrane getting internalized is left unaltered, but the amount of membrane able to reach the endosomal pool is restricted by multiplying with a scaling factor. For eg. A scaling factor of 0.4 means that only 40% of the internalized membrane can reach the endosomal pool, while the rest gets stored in surface connected tubules.

Analysis of endosomes in 3D zstacks over whole cells also provide similar evidence for the effect of deadhesion in Dynasore treated cells. The area fraction of different endosomal compartments is shown in Figure 3.11.

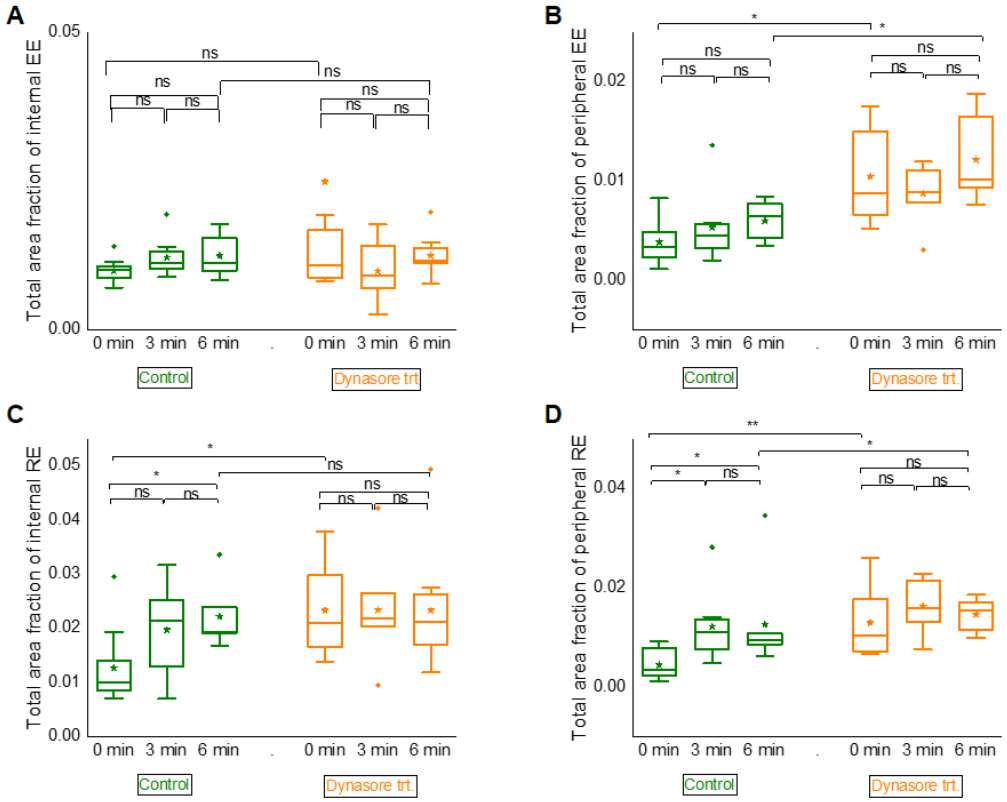

Figure 3.11: Effect of Dynamin Inhibition on trypsinized HeLa cells. HeLa cells were co-transfected with Rab5-EGFP(green) and Rab4-mCherry (red) to mark Early endosomes (EE) and Recycling endosomes (RE), respectively. **(A)** Area fraction of internal EE **(B)** Area fraction of peripheral EE **(C)** Area fraction of internal RE **(D)** Area fraction of peripheral RE **(C)** EE to RE ratio per cell [N_{expt}=1, n_{cells}=8 per sample]

3.5 Effect of Deadhesion in CLIC-GEEC Pathway inhibited Samples

Inhibition of CLIC-GEEC pathway blocks off a large part of endocytic membrane turnover. But, in this case, the dynamin dependant pathways and CME remain active. Inhibition is achieved by treatment with ML141, which is a potent inhibitor of cdc42. cdc42 is necessary for actin assembly in the CLIC-GGEC pathway. So, its inhibition effectively blocks the pathway.

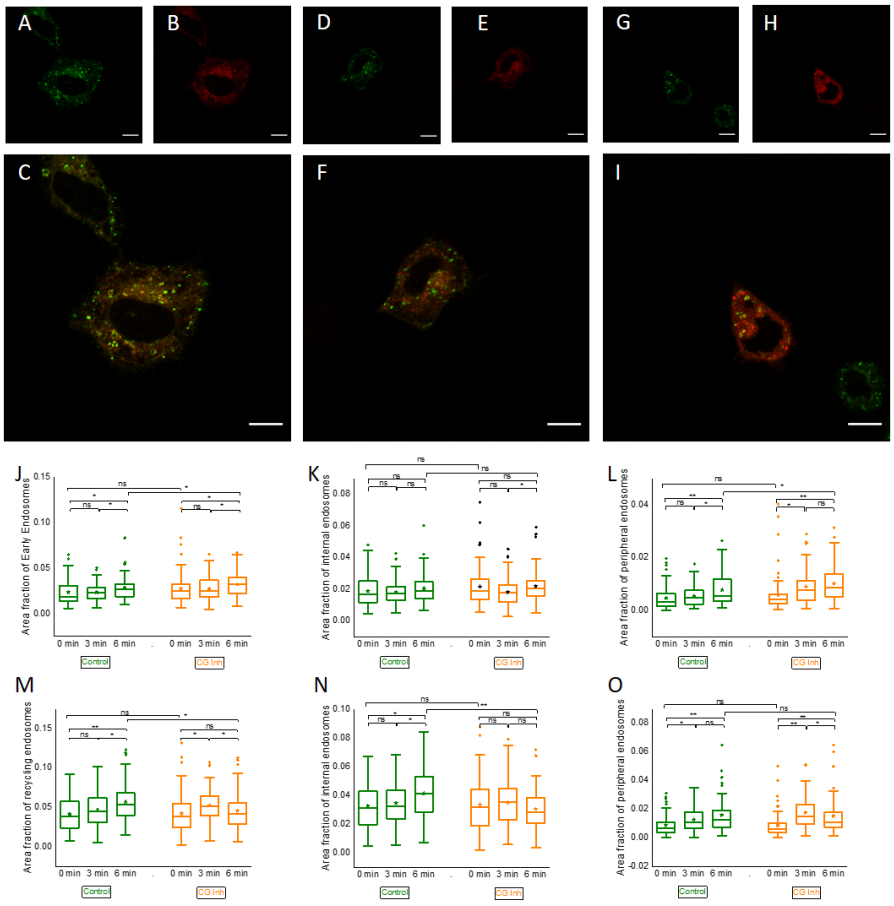

Figure 3.12: Effect of CLIC-GEEC Pathway Inhibition using ML141 on trypsinized HeLa cells. HeLa cells were co-transfected with Rab5-EGFP(green) and Rab4-mCherry (red) to mark Early endosomes (EE) and Recycling endosomes (RE), respectively. Representative images of ML141 treated cells **(A-C)** without trypsin treatment (t=0 min), **(D-F)** with 3 mins trypsin treatment (t=3 min), **(G-I)** with 6 mins trypsin treatment (t=6 min). Images **(C,F,I)** depict merged images from both channels at the three time points. **(J)** Area fraction of total EE **(K)** Area fraction of internal EE **(L)** Area fraction of peripheral EE **(M)** Area fraction of total RE **(N)** Area fraction of internal RE **(O)** Area fraction of peripheral RE. Scale bar: A-10µm (all images) (N_{expt}=3, n_{cells}=50 per sample)

In the initial part of deadhesion (t=0mins to t=3mins), we observe an increase in the peripheral newly formed EE. But, this increase stops and the amount of internal EE is seen to significantly increase in the later part of deadhesion.

Internal REs do not show a significant change during deadhesion, but a large amount of peripheral REs are seen at t=3 min, which then reduces significantly.

This behaviour of early and recycling endosomes closely resembles dynamin inibition. It is so because both dynamin dependent pathways and CLIC-GEEC pathway are major pathways of endocytosis, and their inhibition leads to a large increase in the membrane tension, during deadhesion.

Analysis of endosomes in 3D zstacks for ML141 treated cells is shown in Figure 3.13.

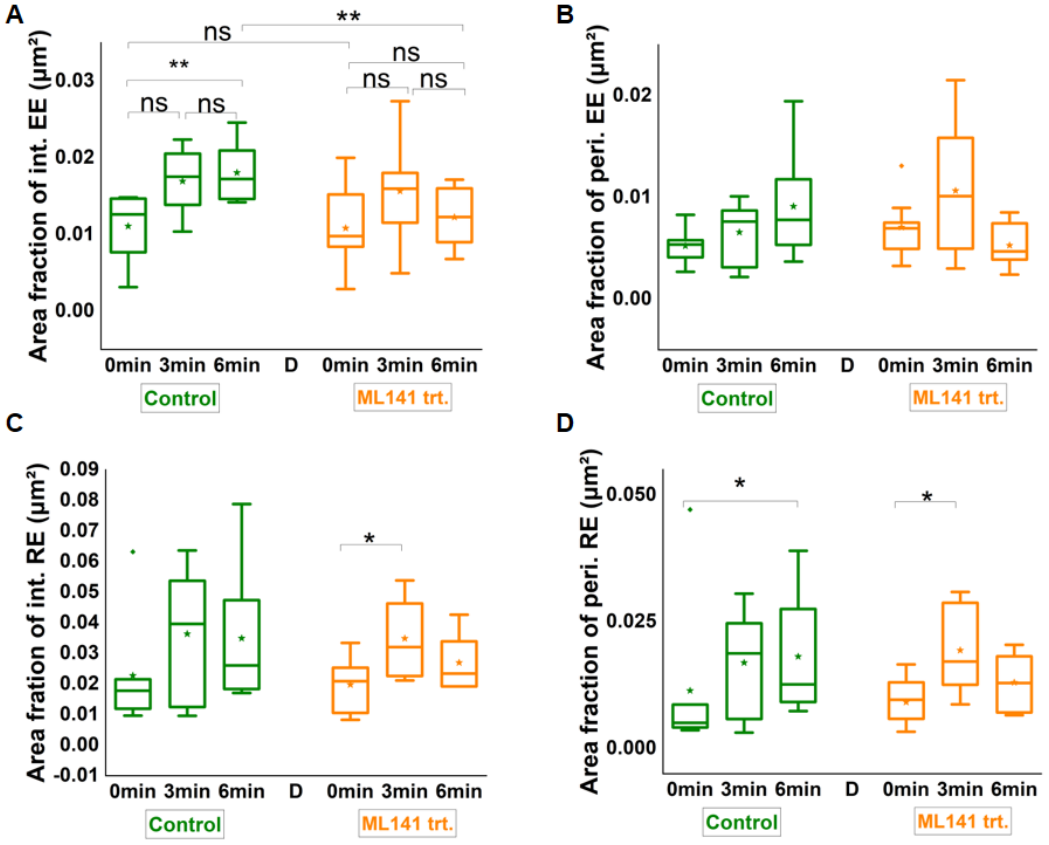

Figure 3.13: Effect of CLIC-GEEC Pathway Inhibition on trypsinized HeLa cells. HeLa cells were co-transfected with Rab5-EGFP(green) and Rab4-mCherry (red) to mark Early endosomes (EE) and Recycling endosomes (RE), respectively. **(A)** Area fraction of internal EE **(B)** Area fraction of peripheral EE **(C)** Area fraction of internal RE **(D)** Area fraction of peripheral RE **(C)** EE to RE ratio per cell [N_{expt}=1, n_{cells}=7 per sample]

Chapter 4

Discussion

HeLa cells were co-transfected with Rab5-EGFP(green) and Rab4-mCherry (red) to mark Early endosomes (EE) and Recycling endosomes (RE), respectively. The cells were treated with trypsin to induce cellular deadhesion and activate the endocytic recycling pathways for surface area regulation. Certain pathways of endocytosis were selectively inhibited by treating the cell with various inhibitors, to gain a better understanding of the recycling machinery.

It is well established that endocytosis increases the membrane tension values by taking extra membrane inside, while exocytosis decreases the tension. This happens as membrane in the form of vesicles get internalized and recycled back to the membrane. In adhered cells, a large percentage of these endosomes are present in the basal part of the cell. However, during deadhesion, most of the endosomes are localized in the peripheral regions of these basal parts of the cell. This is because the effects of deadhesion on the membrane is most prominent in the basal part of the cell, in contact with the substrate.

Cellular deadhesion reduces the membrane tension of the PM due to deposition of excess membrane. So, endocytic recycling is responsible for rectifying this sudden change in tension in an oscillatory manner. This regulation is also largely an ATP-dependent process, requiring energy at nearly all of its steps.

Finally, both dynamin dependent pathways (CME, CavME etc.) and CLIC-GEEC pathway are major pathways of endocytosis, inhibition of which can disrupt the endocytic machinery.

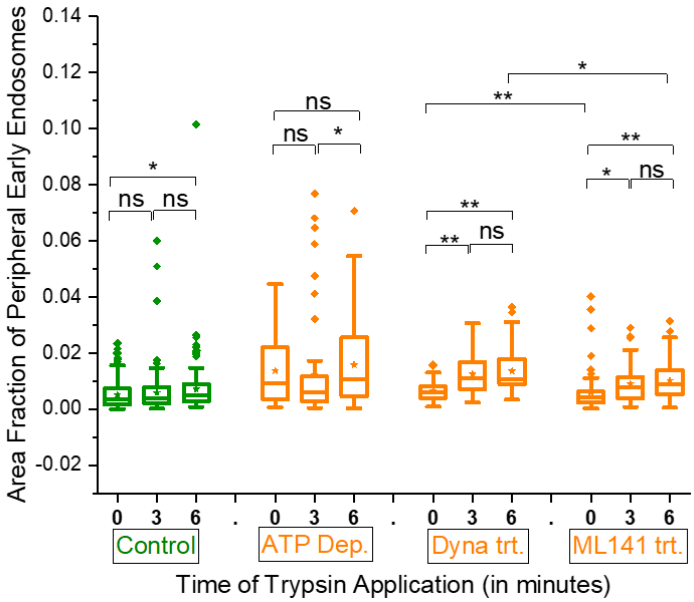

Figure 4.1: Effect of deadhesion on HeLa cells under different conditions [N_{expt}=1, n_{cells}=8 per sample]

Comparing between dynamin inhibition and CLIC-GEEC inhibition, we find that the peripheral EE population in CG inhibited cells is 25± 5% lower in than dynamin inhibited cells. This might suggest that the CG pathway is responsible for a larger fraction of the total amount of endocytosis in deadhering HeLa cells.

Chapter 5

REFERENCES

1. Rebecca Yarwood, John Hellicar, Philip G. Woodman and Martin Lowe. "Membrane trafficking in health and disease", Disease Models & Mechanisms, (2020), 13(4).

2. Peter S. McPherson, Brian K. Kay, Natasha K. Hussain. "Signaling on the Endocytic Pathway", Traffic (Copenhagen, Denmark), (2001), 375–384, 2(6).

3. Bitsikas, Vassilis; Bitsikas, Vassilis; Nichols, Benjamin J. "Clathrin-independent pathways do not contribute significantly to endocytic flux", ELife, (2014), 1–26, 3(3).

4. Rust M, Lakadamyali M, Zhang F, Zhuang X. Assembly of endocytic machinery around individual influenza viruses during viral entry, Nature Structural & Molecular Biology, (2004), 567, 11(6).

5. K Sandvig, B van Deurs. "Endocytosis, intracellular transport, and cytotoxic action of Shiga toxin and ricin", Physiological Reviews, (1996), 949–966, (4).

6. Ronald S Flannagan , Valentin Jaumouillé, Sergio Grinstein. "The cell biology of phagocytosis", Annu Rev Pathol, (2012), 7, 61-98.

7. Teresa Fonovich, Gladis Magnarelli. "Phosphoinositide and phospholipid phosphorylation and hydrolysis pathways—Organophosphate and organochlorine pesticides effects", Advances in Biological Chemistry, 2013 , Vol. 3 No.3A.

8. Mayor, Satyajit; Parton, Robert G.; Donaldson, J. G. "Clathrin-Independent Pathways of Endocytosis", Cold Spring Harbor Perspectives in Biology, (2014), 6(6).

9. Mary J. O'Sullivan and Andrew J. Lindsay. "The Endosomal Recycling Pathway—At the Crossroads of the Cell", Int J Mol Sci., (2020), 6074, 21(17).

10. Elkin, Sarah R.; Lakoduk, Ashley M.; Schmid, Sandra L. "Endocytic Pathways and Endosomal Trafficking: A Primer", Wiener Medizinische Wochenschrift(1946), (2016), 196, 166(7–8).

11. Barth D. Grant & Julie G. Donaldson. "Pathways and mechanisms of endocytic recycling", Nature Reviews. Molecular Cell Biology, (2009), 597, 10(9).

12. Alex H Hutagalung, Peter J Novick. "Role of Rab GTPases in membrane traffic and cell physiology", Physiol Rev., (2011), 91(1), 119–149.

13. Segev, N. "Ypt/rab gtpases: regulators of protein trafficking", Science's STKE: Signal Transduction Knowledge Environment, (2001), (100).

14. Molecular Biology of the Cell, 4th Edition, "Transport into the cell from the Plasma Membrane: Endocytosis".

15. C.E. Morris & U. Homann. "Cell Surface Area Regulation and Membrane Tension", The Journal of Membrane Biology, (2001), 179, 79–102.

16. Chadda R, Howes MT, Plowman SJ, Hancock JF, Parton RG, and Mayor S. "Cholesterol-sensitive Cdc42 activation regulates actin polymerization for endocytosis via the GEEC pathway", Traffic, (2007), 8(6), 702-17.

17. Howes MT, Kirkham M, Riches J, Cortese K, Walser PJ, Simpson F, Hill MM, Jones A, Lundmark R, Lindsay MR, Hernandez-Deviez DJ, Hadzic G, McCluskey A, Bashir R, Liu L, Pilch P, McMahon H, Robinson PJ, Hancock JF, Mayor S, and Parton RG. "Clathrin-independent carriers form a high capacity endocytic sorting system at the leading edge of migrating cells", J Cell Biol, (2010), 190(4), 675–691.

18. Goswami D, Gowrishankar K, Bilgrami S, Ghosh S, Raghupathy R, Chadda R, Vishwakarma R, Rao M, and Mayor S. "Nanoclusters of GPI-anchored proteins are formed by cortical actin-driven activity"

19. Yue, H. Y., Bieberich, E., & Xu, J. "Promotion of endocytosis efficiency through an ATP-independent mechanism at rat calyx of Held terminals.", The Journal of Physiology, (2017), 595(15), 5265

20. Bananis, E., Murray, J. W., Stockert, R. J., Satir, P., & Wolkoff, A. W. "Regulation of early endocytic vesicle motility and fission in a reconstituted system", Journal of Cell Science, (2003), 116(13), 2749–2761. https://doi.org/10.1242/JCS.00478

21. Wucherpfennig, T., Wilsch-Bräuninger, M., & González-Gaitán, M. "Role of Drosophila Rab5 during endosomal trafficking at the synapse and evoked neurotransmitter release", Journal of Cell Biology, (2003), 161(3), 609–624. https://doi.org/10.1083/JCB.200211087<

22. Clathrin-Mediated Endocytosis - Madame Curie Bioscience Database - NCBI Bookshelf, (https://www.ncbi.nlm.nih.gov/books/NBK6479/)

23. Rowland, A. A., Chitwood, P. J., Phillips, M. J., & Voeltz, G. K. "ER Contact Sites Define the Position and Timing of Endosome Fission", Cell, (2014), 159(5), 1027–1041.

24. Stenmark, H. "Rab GTPases as coordinators of vesicle traffic", Nature Reviews Molecular Cell Biology, (2009), 10(8), 513–525.

25. Thottacherry, J. J., Kosmalska, A. J., Kumar, A., Vishen, A. S., Elosegui-Artola, A., Pradhan, S., Sharma, S., Singh, P. P., Guadamillas, M. C., Chaudhary, N., Vishwakarma, R., Trepat, X., del Pozo, M. A., Parton, R. G., Rao, M., Pullarkat, P., Roca-Cusachs, P., & Mayor, S. "Mechanochemical feedback control of dynamin independent endocytosis modulates membrane tension in adherent cells", Nature Communications, (2018), 9(1), 1–14.

26. Djakbarova, U., Madraki, Y., Chan, E. T., & Kural, C. "Dynamic interplay between cell membrane tension and clathrin-mediated endocytosis", Biology of the Cell, (2021), 113(8), 344–373.

27. Gauthier, N. C., Rossier, O. M., Mathur, A., Hone, J. C., & Sheetz, M. P. "Plasma Membrane Area Increases with Spread Area by Exocytosis of a GPI-anchored Protein Compartment", (2009), doi.org/10.1091/MBC.E09-01-0071

28. Bastin, G., & Heximer, S. P. "Rab Family Proteins Regulate the Endosomal Trafficking and Function of RGS4", The Journal of Biological Chemistry, (2013), 288(30), 21836.

29. H. Steven Wiley and Dennis D. Cunningham. "The Endocytotic Rate Constant", THE JOURNAL OF BIOLOGICAL CHEMISTRY, (1982), 257(8).

30. D J Weaver Jr, E W Voss Jr. "Analysis of rates of receptor-mediated endocytosis and exocytosis of a fluorescent hapten-protein conjugate in murine macrophage: implications for antigen processing", J Biol Cell, (1998), 90(2), 169-81

31. Marc R. Birtwistle & Boris N. Kholodenko. "Endocytosis and signalling: A meeting with mathematics", Molecular Oncology, (2009), 3(4), 308-320.

32. Caspar T. H. Jonker, Claire Deo, Patrick J. Zager, Ariana N. Tkachuk, Alan M. Weinstein, Enrique Rodriguez-Boulan, Luke D. Lavis & Ryan Schreiner. "Accurate measurement of fast endocytic recycling kinetics in real time", J Cell Sci, (2020), 133(2).

33. Stephen A.Morris & Sandra L.Schmid. "Synaptic Vesicle Recycling: The Ferrari of endocytosis?", Current Biology, (1995), 5(2), 113-115.

Chapter 6

Appendix

6.1 MATLAB Code for Endosome Counting

```
foldername = 'D:\thesis_data\CGI\t6\9\egfp'


y = myfunc(foldername);
%imgsuffix = '_egfp.tif'


function final = myfunc(filename)
    num_images = 35
    for i = 1:num_images
        imgname = '9'
        imgname1 = append(imgname, '.lsm_')
        roiimgname1 = append(imgname, '\roi')
        roiimgname2 = append(imgname, '\roi2')
        imgid = num2str(i);
        preimgfilename = append(char(imgid),'_egfp.tif');
        imgfilename = append(imgname1, preimgfilename)
        %imgfilename = append(char(imgid),'_af168.tif');
        %imgfilename = '1_af168.tif';
        fullfilename = fullfile(filename, imgfilename);
        id = filename(end-9:end-8);
```

```
I = imread(fullfilename);
%imtool(I)
Iblur = imgaussfilt(I,5);
denoisedImage = (I - Iblur);
normImage1 = mat2gray(denoisedImage);
BW1 = im2bw(normImage1,0.07);
%imtool(BW1);

roi = regionprops('table',BW1,'Centroid');
roifoldername = append('D:\thesis_data\CGI\t6\', roiimgname1);
%roifoldername = 'D:\thesis_data\snaps';
roilastname = append(char(imgid),'.roi');
roifilename = fullfile(roifoldername, roilastname);

roi2 = regionprops('table',BW1,'Centroid');
roifoldername2 = append('D:\thesis_data\CGI\t6\',roiimgname2);
roilastname2 = append(char(imgid),'.roi');
roifilename2 = fullfile(roifoldername2, roilastname2);

[sROI] = ReadImageJROI(roifilename);
T = struct2cell(sROI);
M = cell2mat(T(7));
x = M(:,1);
y = M(:,2);
BW = roipoly(I,x,y);
bmask = boundarymask(BW);
%imtool(BW);
%imtool(bmask);

[sROI2] = ReadImageJROI(roifilename2);
T2 = struct2cell(sROI2);
M2 = cell2mat(T2(7));
x2 = M2(:,1);
```

```
y2 = M2(:,2);
BW2 = roipoly(I,x2,y2);
bmask2 = boundarymask(BW2);
%imtool(BW2);

ROI_sel = BW1;
ROI_sel(BW == 0) = 0;
%imtool(ROI_sel);

ROI_sel2 = ROI_sel;
ROI_sel2(BW2 == 1) = 0;
%imtool(ROI_sel2);

SE = strel("disk",1);
a1 = imerode(ROI_sel,SE);
b1 = imdilate(a1,SE);
final = imfuse(bmask,b1);
finalx = imfuse(bmask2,final);
%imtool(finalx);

SE2 = strel("disk",1);
a2 = imerode(ROI_sel2,SE2);
b2 = imdilate(a2,SE);
final2 = imfuse(bmask,b2);
final2x = imfuse(bmask2,final2);
%imtool(b1);
%imtool(b2);

finalim = imfuse(finalx,I);
%imtool(finalim);

finalim2 = imfuse(final2x,I);
%imtool(finalim2);
```

```
%saveimgop = montage({I,final})
imgsavename = append(char(imgid),'.tif');
imgsavename1 = fullfile('endosomes_pi\ee',imgsavename);
imwrite(finalim, imgsavename1)

props1 = regionprops(BW, 'Area', 'Perimeter');
cellAreas = [props1.Area]*0.166*0.166;

props = regionprops(b1, 'Area', 'Perimeter');
allAreas = [props.Area];
areaum = allAreas * 0.166 * 0.166;
totalArea = sum(areaum);
endo_num = size(areaum);
numdensity = endo_num(2) / cellAreas(1);
areadensity = totalArea / cellAreas(1);
allPerimeters = [props.Perimeter];
circularity = (allPerimeters .^ 2) ./ (4 * pi * allAreas);
avgendoarea = mean(areaum);
avgendocirc = mean(circularity);

props_peri = regionprops(b2, 'Area', 'Perimeter');
allAreas_peri = [props_peri.Area];
areaum_peri = allAreas_peri * 0.166 * 0.166;
totalArea_peri = sum(areaum_peri);
endo_num_peri = size(areaum_peri);
numdensity_peri = endo_num_peri(2) / cellAreas(1);
areadensity_peri = totalArea_peri / cellAreas(1);
allPerimeters_peri = [props_peri.Perimeter];
circularity_peri = (allPerimeters_peri .^ 2) ./ (4 * pi * allAreas_peri);
avgendoarea_peri = mean(areaum_peri);
avgendocirc_peri = mean(circularity_peri);
```

```
totalArea_int = totalArea - totalArea_peri;
endo_num_int = endo_num(2) - endo_num_peri(2);
numdensity_int = endo_num_int / cellAreas(1);
areadensity_int = totalArea_int / cellAreas(1);

peri_total_ratio = totalArea_peri / totalArea
int_total_ratio = totalArea_int / totalArea
peri_int_ratio = totalArea_peri / totalArea_int



datamain = cat(2,transpose(areaum),transpose(circularity));
data2 = cat(2, avgendoarea, totalArea, avgendocirc, cellAreas(1),
endo_num(2), areadensity, numdensity

%data3 = cat(2, totalArea_peri,endo_num_peri(2),numdensity_peri,
areadensity_peri,avgendoarea_peri,avgendocirc_peri,totalArea_int,
endo_num_int,numdensity_int,areadensity_int,peri_total_ratio,
int_total_ratio,peri_int_ratio)

data3 = cat(2, avgendoarea, totalArea, avgendocirc, cellAreas(1),
endo_num(2), areadensity, numdensity, totalArea_peri, endo_num_peri(2),
numdensity_peri, areadensity_peri, avgendoarea_peri, avgendocirc_peri,
totalArea_int, endo_num_int, numdensity_int, areadensity_int,
peri_total_ratio, int_total_ratio, peri_int_ratio);

%output1 = append('data_c_',char(imgid));
%output = append(output1,'.csv');
%%csvwrite(output,datamain)

labels_data3 = {'avgendoarea ', 'totalArea ', 'avgendocirc ',
'cellAreas ', 'endo_num ', 'areadensity ', 'numdensity ',
'totalArea_peri ', 'endo_num_peri ', 'numdensity_peri ',
```

```
        'areadensity_peri ', 'avgendoarea_peri ', 'avgendocirc_peri ',
        'totalArea_int ', 'endo_num_int ', 'numdensity_int ','areadensity_int ',
        'peri_total_ratio ', 'int_total_ratio ', 'peri_int_ratio '};

        output = 'data_ee_extended.csv';
        %output2 = 'summary.csv';
        output3 = 'summary_ee_extended.csv'
        %dlmwrite(output,datamain,'-append', 'roffset', 1, 'coffset', 0);
        %dlmwrite(output2,data2,'-append');
        %dlmwrite(output3,labels_data3,'-append','delimiter','');
        dlmwrite(output3,data3,'-append');
    end
end
```

6.2 MATLAB Code for Colocalization Analysis

Colocalization analysis involves both codes given below:

1. Binary Maker

```
foldername = 'D:\thesis_data\new_analysis\coloc_analysis\cgi\t0\8\egfp'


y = myfunc(foldername);
y1 = myfunc2(foldername2);
%imgsuffix = '_egfp.tif'


function final = myfunc(filename)
    num_images = 26
    for i = 1:num_images
        imgname = '8'
        %imgnametemp = append('_', imgname)
        imgname1 = append(imgname, '.lsm')
        roiimgname1 = append(imgname, '\roi')
        imgid = num2str(i);
        preimgfilename = append(num2str(i),'_egfp.tif');
        imgfilename1 = append('_', preimgfilename)
        imgfilename = append(imgname1,imgfilename1)
        %imgfilename = append(char(imgid),'_af168.tif');
        %imgfilename = '1_af168.tif';
        fullfilename = fullfile(filename, imgfilename);
        id = filename(end-9:end-8);



        I = imread(fullfilename);
        %imtool(I)
        Iblur = imgaussfilt(I,5);
        denoisedImage = (I - Iblur);
        normImage1 = mat2gray(denoisedImage);
        BW1 = im2bw(normImage1,0.07);
```

```
%imtool(BW1);

roi = regionprops('table',BW1,'Centroid');
roifoldername = append('D:\thesis_data\coloc_analysis\', roiimgname1);

%roifoldername = 'D:\thesis_data\snaps';
roilastname = append(char(imgid),'.roi');
roifilename = fullfile(roifoldername, roilastname);

[sROI] = ReadImageJROI(roifilename);
sROI;
T = struct2cell(sROI);
M = cell2mat(T(7));
x = M(:,1);
y = M(:,2);
BW = roipoly(I,x,y);
bmask = boundarymask(BW);
%imtool(BW);

ROI_sel = BW1;
ROI_sel(BW == 0) = 0;
%imtool(ROI_sel);

SE = strel("disk",1);
a1 = imerode(ROI_sel,SE);
b1 = imdilate(a1,SE);
final = imfuse(bmask,b1);
%imtool(b1);

imgsavename = append(char(imgid),'.tif');
imgsavename1 = fullfile('endosomes\ee',imgsavename);
imwrite(b1, imgsavename1);
```

```
        props = regionprops(b1, 'Area', 'Perimeter');
        allAreas = [props.Area];
        areaum = allAreas * 0.166 * 0.166;
        totalArea = sum(areaum);
        endo_num = size(areaum);

        datax = cat(2, totalArea, endo_num)
        output2 = 'coloc-test.csv';
        %dlmwrite(output,datamain,'-append', 'roffset', 1, 'coffset', 0);
        %dlmwrite(output2,datax,'-append');
    end
end
```

2. Colocalization Finder

```
foldername = 'C:\Users\aritr\Desktop\temp_celldata\endosomes\ee';
foldername2 = 'C:\Users\aritr\Desktop\temp_celldata\endosomes\re';

for i = 1:26
    imgname1 = append(num2str(i), '.tif');
    %roiimgname1 = append(imgname, '\roi')
    imgid = num2str(i);
    %preimgfilename = append(char(imgid),'_egfp.tif');
    %preimgfilename2 = append(char(imgid),'_af168.tif');
    %imgfilename = append(imgname1, preimgfilename);
    %imgfilename2 = append(imgname1, preimgfilename2);
    fullfilename = fullfile(foldername, imgname1);
    fullfilename2 = fullfile(foldername2, imgname1);


    I1 = imread(fullfilename);
    I2 = imread(fullfilename2);

    %imshow(I1);
```

```
    %imshow(I2);

    K = and(I1, I2);
    %imshow(K);

    imgsavename = append(char(imgid),'.tif');
    imgsavename1 = fullfile('endosomes\coloc',imgsavename);
    imwrite(K, imgsavename1);

    props = regionprops(K, 'Area');
    allAreas = [props.Area];
    areaum = allAreas * 0.166 * 0.166;
    colocArea = sum(areaum);
    endo_num = size(areaum);

    props = regionprops(I1, 'Area');
    allAreas = [props.Area];
    areaum = allAreas * 0.166 * 0.166;
    EEArea = sum(areaum);

    props = regionprops(I2, 'Area');
    allAreas = [props.Area];
    areaum = allAreas * 0.166 * 0.166;
    REArea = sum(areaum);

    datax = cat(2, endo_num(2), colocArea, EEArea, REArea);
    output2 = 'coloc-test-AND.csv';
    dlmwrite(output2,datax,'-append');
end
```

6.3 ImageJ Macros

6.3.1 Macro to split .lsm files and convert to .tif

```
    macro batch_save_image_sequence{
dir1 = getDirectory("Choose source directory");
list = getFileList(dir1);

Array.print(list);
arr_num= extract_digits(list);
Array.sort(arr_num, list);
Array.print(list);

setBatchMode(true);
for (i=0; i<list.length; i++) {
m = toString(i+1)+".lsm";
print(m);
print(list[i]);
print(dir1+list[i]);
open(dir1+list[i]+m);
getDimensions(width, height, channels, slices, frames);
counter=1;
title = File.nameWithoutExtension;
for (j=1; j<=slices; j++){
run("Make Substack...", "channels=1-"+channels+" slices="+j);
saveAs("tif", dir1+list[i]+m+"_"+counter+".tif");
close();
counter+=1;
}
}
close();

//Numerical Sorting Function
//Usage:
```

```
//num_sort= extract_digits(input);
//Array.sort(num_sort, input);

function extract_digits(a) {
arr2 = newArray; //return array containing digits
for (i = 0; i < a.length; i++) {
str = a[i];
digits = "";
for (j = 0; j < str.length; j++) {
ch = str.substring(j, j+1);
if(!isNaN(parseInt(ch)))
digits += ch;
}
arr2[i] = parseInt(digits);
}
return arr2;
}
```

6.3.2 Macro to split multichannel .tif files

```
    dir=getDirectory("Choose a Directory");
print(dir);
splitDir1= dir + "/egfp/";
splitDir2= dir + "/af168/";
splitDir3= dir + "/dic/";
File.makeDirectory(splitDir1);
File.makeDirectory(splitDir2);
File.makeDirectory(splitDir3);
list = getFileList(dir);

for (i=0; i<list.length; i++) {
     if (endsWith(list[i], ".tif")){
               print(i + ": " + dir+list[i]);
```

```
            open(dir+list[i]);
            imgName=getTitle();
        baseNameEnd=indexOf(imgName, ".tif");
        baseName=substring(imgName, 0, baseNameEnd);
        run("Split Channels");
        selectWindow("C1-" + imgName);
        saveAs("Tiff",  splitDir1 + baseName +  "_egfp.tif");
        selectWindow("C2-" + imgName);
        saveAs("Tiff",  splitDir2 + baseName +  "_af168.tif");
        selectWindow("C3-" + imgName);
        saveAs("Tiff",  splitDir3 + baseName +  "_dic.tif");
        run("Close All");
    } else {
    write("One Channel Conversion is Complete");
    }
}
```